

## Transient analysis of cross-ply laminated shells using FSDT: Alternative formulation

Mehmet Fatih Sahan \*

*Department of Civil Engineering, Adiyaman University, 02040 Adiyaman, Turkey*

*(Received March 07, 2014, Revised June 02, 2014, Accepted September 29, 2014)*

**Abstract.** This paper aims to present an alternative analytical method for transient vibration analysis of doubly-curved laminated shells subjected to dynamic loads. In the method proposed, the governing differential equations of laminated shell are derived using the dynamic version of the principle of virtual displacements. The governing equations of first order shear deformation laminated shell are obtained by Navier solution procedure. Time-dependent equations are transformed to the Laplace domain and then Laplace parameter dependent equations are solved numerically. The results obtained in the Laplace domain are transformed to the time domain with the help of modified Durbin's numerical inverse Laplace transform method. Verification of the presented method is carried out by comparing the results with those obtained by Newmark method and ANSYS finite element software. Also effects of number of laminates, different material properties and shell geometries are discussed. The numerical results have proved that the presented procedure is a highly accurate and efficient solution method.

**Keywords:** doubly-curved laminated shell; transient vibration analysis; inverse laplace transform; analytic solution

---

### 1. Introduction

Laminated composite shells are being increasingly used in all fields of engineering because of their many advantageous properties. The most advantageous part of shell structures is their load-carrying ability due to combination of laminates and their curvature. Therefore, many papers have been published on this subject. Transient vibration analysis of shells made of layers has a primary importance engineering design. It is necessary to have a full understanding of the behavior of laminated composite shells. Researchers have been attempted to estimate exactly the stress distribution and displacement varying with time under various dynamic loading conditions.

Many investigators have studied the free vibration of laminated shell structures based on first order shear deformation theory (FSDT) or higher order (Civalek 2006, Dogan and Arslan 2012, Lee *et al.* 2003, Timarci and Soldatos 2000, Topal 2013). Toh *et al.* (1995) examined the transient stress response of an orthotropic laminated open cylindrical shell. They presented the solution analytically which includes both contact deformation and transverse shear. Shim *et al.* (1996) examined analytically the elastic response of glass/epoxy laminated composite shells subjected to

---

\*Corresponding author, Assistant Professor, E-mail: [mfs@adiyaman.edu.tr](mailto:mfs@adiyaman.edu.tr)

low velocity impact. Gong *et al.* (1995) presented a set of analytical solutions to predict the dynamic response of simply supported laminated shells. Wu *et al.* (1996) formulated an asymptotic theory for dynamic analysis of doubly curved laminated shells within the framework of three-dimensional elasticity. Chun and Lam (1995) investigated the free and forced vibration of laminated curved panels subjected to the triangular, explosive and step loadings. The Rayleigh-Ritz method is employed to achieve the natural frequencies of the clamped laminated curved panels. The normal mode superposition method is used in the forced vibration analysis. Vaziri *et al.* (1996) showed a series of outcomes for the non-penetrating, low velocity impact response of cylindrical shells using super finite element method. For the time integration, the Newmark scheme and the Newton-Raphson method are employed. Prusty and Satsangi (2001) described the transient response of composite stiffened plates and shells. The governing undamped equation of motion are obtained with finite element method and Newmark's method is used for the direct time integration. Swaddiwudhipong and Lui (1997) used modified nine-node degenerated shell elements to investigate the elastic and elasto-plastic dynamic response of laminated composite plate and shell structures. In his study, Newmark's algorithm is used for the direct time integration. Ganapathi *et al.* (2002) presented finite element procedure for transient response of laminated cross-ply cylindrical shells subjected to thermal/mechanical loads based on a higher-order shear deformation theory. The shell responses are determined employing finite element approach in connection with a direct time integration technique. Krishnamurthy *et al.* (2001) studied the impact response and the resulting damage of laminated composite shell objects by a metallic impactor via the finite-element approach. The equations are solved by way of the Hughes and Liu predictor-corrector adaptation of the Newmark's procedure. Krishnamurthy *et al.* (2003) used the finite element methods and the classical Fourier series to obtain impact response of a laminated composite cylindrical shell. Equations are solved by means of Newmark's algorithm combined with a predictor-corrector scheme. Her and Liang (2004) studied the composite laminate and shell structures subjected to low velocity impact by the ANSYS/LSDYNA finite element software. Park *et al.* (2005) presented static and dynamic analysis of composite plates and shells. The transverse shear stiffness was defined by an equilibrium approach. To determine the element stiffness matrix, the Quasi-Conforming Technique was used. Newmark-b method was used for time integration. Saviz and Muhammadpourfad (2010) presented elasticity solution of a cross-ply laminated cylindrical shell with piezoelectric layer subjected to dynamic local loading. Galerkin's finite element method is used in radial direction. The static finite element matrix equations are used to obtain the implicit Newmark method. Jung and Han (2014) investigated the vibration analysis of functionally graded material and laminated composite structures, using a refined 8-node shell element that allows for the effects of transverse shear deformation and rotary inertia. For the study, the Newmark-b time integration method was adopted. Corriera *et al.* (2000) presented a numerical method for the structural analysis of laminated axisymmetric shells based on the high-order theory. Sofiyev (2003) considered torsional buckling of cross-ply laminated orthotropic composite cylindrical thin shells under loads, which is a power function of time. The modified Donnell type dynamic stability and compatibility equations were obtained first. Then applying Galerkin's method to the equations are reduced to a time dependent differential equation. Fares *et al.* (2003) used a design control optimization approach to determine optimal levels of ply thickness, fiber orientation angle and closed loop control force for composite laminated doubly curved shells based on a higher-order shell theory. Li and Hua (2009) solved the problem of the transient vibration of an elastic laminated composite cylindrical shell with infinite length exposed to an underwater shock wave, approximately. The Sanders thin shell theory was

used to obtain governing equations of motion of the shell. The application of the RAVS approximation to obtain the transient responses of the composite cylindrical shells exposed to underwater shocks was demonstrated by using the finite difference method.

As noted above, numerical solutions of doubly-curved laminated shells are generally achieved using Newmark method. The literature for the transient analysis of doubly curved laminated shells in the Laplace domain is very limited. Nevertheless, to the best of present authors' knowledge the transient vibration of doubly-curved orthotropic laminated shells using the Navier procedure in connection with the Laplace transforms has not been published yet. In this study, the application of a simple and an efficient method to the transient vibration analysis of doubly-curved laminated shells base on FSDT will be introduced.

In the present paper, the dynamic analysis of doubly curved laminated shells is examined theoretically with the Laplace transform. The governing differential equations of laminated shell are derived using the dynamic version of the principle of virtual displacements. The laminated shell formulations are based on FSDT. Closed-form expressions of the system of differential equations of dynamic equilibrium are obtained with the Navier solution procedure. After considering initial condition and applying Laplace transform on the governing equations of motion the linear algebraic equations are obtained. Equations in the Laplace domain are solved numerically by Gauss elimination method for a sequence of values of Laplace parameter. Use of Laplace transform has the advantage that the dynamic system is efficiently reduced to a static one. Dynamic forces or displacements of any time variation can be determined without any adversity by employing a direct numerical Laplace transform. Then, the solutions obtained in the Laplace domain are transformed to the real time with the help of the modified Durbin's inverse Laplace transform method (Durbin 1974, Narayanan 1979, Sahan 2012, Temel 2003, Temel and Şahan 2013a, b). To verify the numerical results obtained with presented procedure are compared with those obtained with semi-analytical method and ANSYS finite element software. In the semi-analytical method closed-form expressions of the governing equation of dynamic equilibrium were achieved using the Navier approach and the Newmark method was operated for time integration. Dynamic results are presented for doubly curved laminated shells with simply

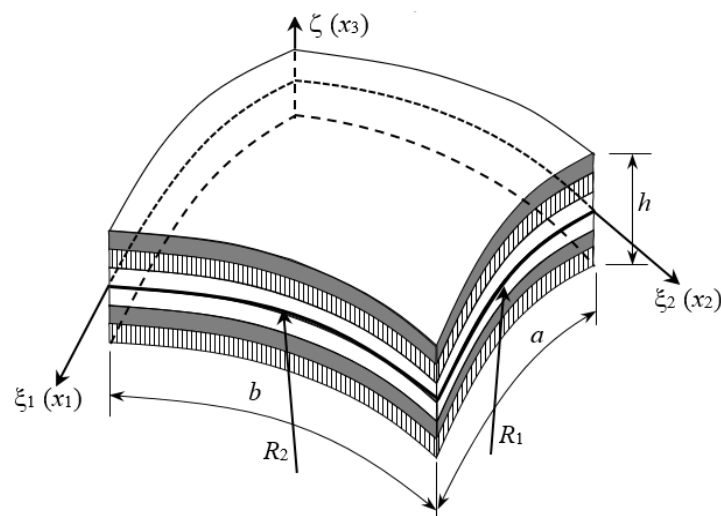


Fig. 1 Coordinate and Geometry of a doubly-curved shell

supported boundary conditions. Also effects of number of laminates, different material properties and shell geometries on the transient response of shells are discussed. The results obtained with the suggested method are found to be in excellent agreement with those in the literature.

Obtaining the equation of doubly curved laminated shells first in the time domain by Navier approach then applying Laplace transform to the governing equations and finally transforming results to the time domain via inverse Laplace method has proved to be a highly accurate and effective approach when compared to other numerical techniques in the literature.

## 2. Theory and formulation of laminated shell

Suppose that the shell is composed of  $N$  orthotropic layers of uniform thickness. Co-ordinate system of doubly curved laminated shell is shown in Fig. 1. Here, an orthogonal curvilinear coordinate system is composed from  $\xi_1$ ,  $\xi_2$ ,  $\zeta$  coordinates.  $\xi_1$  and  $\xi_2$  curves are lines of curvature on the mid-surface of the shell.

### 2.1 Kinematics of the shell

The displacement field based on FSDT of thick shells is defined as (Reddy 2004)

$$\begin{Bmatrix} u_1(\xi_1, \xi_2, \zeta, t) \\ v_2(\xi_1, \xi_2, \zeta, t) \\ w_3(\xi_1, \xi_2, \zeta, t) \end{Bmatrix} = \begin{Bmatrix} u_0(\xi_1, \xi_2, t) \\ v_0(\xi_1, \xi_2, t) \\ w_0(\xi_1, \xi_2, t) \end{Bmatrix} + \zeta \begin{Bmatrix} \varnothing_1(\xi_1, \xi_2, t) \\ \varnothing_2(\xi_1, \xi_2, t) \\ 0 \end{Bmatrix} \quad (1)$$

where  $(u_1, u_2, u_3)$  are the displacements of a point  $(\xi_1, \xi_2, \zeta)$  in the laminated plate,  $(u_0, v_0, w_0)$  are the displacements of a point  $(\xi_1, \xi_2, 0)$  on the mid-surface of the shell.  $(\varnothing_1, \varnothing_2)$  are the rotations of the reference surface,  $\zeta = 0$ , about the  $\xi_2$ - and  $\xi_1$ - coordinate axes, respectively. By substitution of the displacement relations given by Eq. (1) into the linear strain displacement equations of the theory of elasticity, the following relations are obtained (Reddy 1984).

$$\begin{aligned} \{\varepsilon\} &= \{\varepsilon^0\} + \zeta \{\kappa\}, \quad \{\gamma\} = \{\gamma_{23}, \gamma_{13}\}^T \\ \{\varepsilon\} &= \{\varepsilon_1, \varepsilon_2, \gamma_{12}\}^T, \quad \{\varepsilon^0\} = \{\varepsilon_1^0, \varepsilon_2^0, \gamma_{12}^0\}^T, \quad \{\kappa\} = \{\kappa_1, \kappa_2, \kappa_3\}^T \end{aligned} \quad (2)$$

$$\begin{aligned} \varepsilon_1^0 &= \frac{1}{\alpha_1} \frac{\partial u_0}{\partial \xi_1} + \frac{w_0}{R_1}, \quad \varepsilon_2^0 = \frac{1}{\alpha_2} \frac{\partial v_0}{\partial \xi_2} + \frac{w_0}{R_2}, \quad \gamma_{12}^0 = \frac{1}{\alpha_1} \frac{\partial v_0}{\partial \xi_1} + \frac{1}{\alpha_2} \frac{\partial u_0}{\partial \xi_2} \\ \gamma_{23} &= \frac{1}{\alpha_2} \frac{\partial w_0}{\partial \xi_2} + \varnothing_2 - \frac{v_0}{R_2}, \quad \gamma_{13} = \frac{1}{\alpha_1} \frac{\partial w_0}{\partial \xi_1} + \varnothing_1 - \frac{u_0}{R_1} \\ \kappa_1 &= \frac{1}{\alpha_1} \frac{\partial \varnothing_1}{\partial \xi_1}, \quad \kappa_2 = \frac{1}{\alpha_2} \frac{\partial \varnothing_2}{\partial \xi_2}, \quad \kappa_3 = \frac{1}{\alpha_1} \frac{\partial \varnothing_2}{\partial \xi_1} + \frac{1}{\alpha_2} \frac{\partial \varnothing_1}{\partial \xi_2} + \frac{1}{2} \left( \frac{1}{R_2} - \frac{1}{R_1} \right) \left( \frac{1}{\alpha_1} \frac{\partial v_0}{\partial \xi_1} - \frac{1}{\alpha_2} \frac{\partial u_0}{\partial \xi_2} \right) \end{aligned} \quad (3)$$

### 2.2 Constitutive equations

Composite shell layers stacked on each other with the principal material 1 axis of the  $k$ th layer is oriented at an angle  $\theta^{(k)}$  from the shell  $x_1$  coordinate in the counterclockwise sense and  $x_3^{(k)} = \zeta$ . The stress-strain relations of the  $k$ th orthotropic lamina in the shell coordinate system are given as

$$\begin{Bmatrix} \sigma_{11} \\ \sigma_{22} \\ \tau_{12} \\ \tau_{23} \\ \tau_{13} \end{Bmatrix}^{(k)} = \begin{bmatrix} \bar{Q}_{11} & \bar{Q}_{12} & \bar{Q}_{16} & 0 & 0 \\ \bar{Q}_{12} & \bar{Q}_{22} & \bar{Q}_{26} & 0 & 0 \\ \bar{Q}_{16} & \bar{Q}_{26} & \bar{Q}_{66} & 0 & 0 \\ 0 & 0 & 0 & \bar{Q}_{44} & \bar{Q}_{45} \\ 0 & 0 & 0 & \bar{Q}_{45} & \bar{Q}_{55} \end{bmatrix}^{(k)} \begin{Bmatrix} \varepsilon_{11} \\ \varepsilon_{22} \\ \gamma_{12} \\ \gamma_{23} \\ \gamma_{13} \end{Bmatrix} \quad (4)$$

where  $\bar{Q}_{ij}$  are the transformed stiffnesses, and  $Q_{ij}^{(k)}$  are the lamina stiffnesses referred to the principal material coordinates of the  $k$ th laminad

$$\begin{aligned} \bar{Q}_{11} &= Q_{11}^{(k)} \cos^4 \theta^{(k)} + 2(Q_{12}^{(k)} + 2Q_{66}^{(k)}) \sin^2 \theta^{(k)} \cos^2 \theta^{(k)} + Q_{22}^{(k)} \sin^4 \theta^{(k)} \\ \bar{Q}_{12} &= (Q_{11}^{(k)} + Q_{22}^{(k)} - 4Q_{66}^{(k)}) \sin^2 \theta^{(k)} \cos^2 \theta^{(k)} + Q_{12}^{(k)} (\sin^4 \theta^{(k)} + \cos^4 \theta^{(k)}) \\ \bar{Q}_{22} &= Q_{11}^{(k)} \sin^4 \theta^{(k)} + 2(Q_{12}^{(k)} + 2Q_{66}^{(k)}) \sin^2 \theta^{(k)} \cos^2 \theta^{(k)} + Q_{22}^{(k)} \cos^4 \theta^{(k)} \\ \bar{Q}_{16} &= (Q_{11}^{(k)} - Q_{22}^{(k)} - 2Q_{66}^{(k)}) \sin \theta^{(k)} \cos^3 \theta^{(k)} + (Q_{12}^{(k)} - Q_{22}^{(k)} + 2Q_{66}^{(k)}) \sin^3 \theta^{(k)} \cos \theta^{(k)} \\ \bar{Q}_{26} &= (Q_{11}^{(k)} - Q_{12}^{(k)} - 2Q_{66}^{(k)}) \sin^3 \theta^{(k)} \cos \theta^{(k)} + (Q_{12}^{(k)} - Q_{22}^{(k)} + 2Q_{66}^{(k)}) \sin \theta^{(k)} \cos^3 \theta^{(k)} \\ \bar{Q}_{66} &= (Q_{11}^{(k)} + Q_{22}^{(k)} - 2Q_{12}^{(k)} - 2Q_{66}^{(k)}) \sin^2 \theta^{(k)} \cos^2 \theta^{(k)} + Q_{66}^{(k)} (\sin^4 \theta^{(k)} + \cos^4 \theta^{(k)}) \\ \bar{Q}_{44} &= Q_{44}^{(k)} \cos^2 \theta^{(k)} + Q_{55}^{(k)} \sin^2 \theta^{(k)} \\ \bar{Q}_{45} &= (Q_{55}^{(k)} - Q_{44}^{(k)}) \sin \theta^{(k)} \cos \theta^{(k)} \\ \bar{Q}_{55} &= Q_{55}^{(k)} \cos^2 \theta^{(k)} + Q_{44}^{(k)} \sin^2 \theta^{(k)} \end{aligned} \quad (5)$$

$$\begin{aligned} Q_{11}^{(k)} &= \frac{E_1^{(k)}}{(1 - \nu_{12}^{(k)} \nu_{21}^{(k)})}, & Q_{12}^{(k)} &= \frac{\nu_{12}^{(k)} E_2^{(k)}}{(1 - \nu_{12}^{(k)} \nu_{21}^{(k)})}, & Q_{22}^{(k)} &= \frac{E_2^{(k)}}{(1 - \nu_{12}^{(k)} \nu_{21}^{(k)})} \\ Q_{66}^{(k)} &= G_{22}^{(k)}, & Q_{44}^{(k)} &= G_{23}^{(k)}, & Q_{55}^{(k)} &= G_{13}^{(k)} \end{aligned} \quad (6)$$

where  $E_i^{(k)}$  denotes Young's modulus of the  $k$ th lamina in the  $i$ -th material direction of elasticity,  $\nu_{ij}^{(k)}$  Poisson's ratio for transverse strain of the  $k$ th lamina in the  $j$ -th direction when stressed in the  $i$ -th direction and  $G_{ij}^{(k)}$  are shear modulus of the  $k$ th lamina in the  $i$ - $j$  planes.

Based on the FSDT shell, in-plane force resultants ( $N_{11}$ ,  $N_{22}$ ,  $N_{12}$ ), moment resultants ( $M_{11}$ ,  $M_{22}$ ,  $M_{12}$ ) and transverse force resultants ( $Q_1$ ,  $Q_2$ ) are defined as

$$\begin{aligned}
\{N\} &= \begin{Bmatrix} N_{11} \\ N_{11} \\ N_{12} \end{Bmatrix} = \sum_{k=1}^N \int_{\zeta_k}^{\zeta_{k+1}} \begin{Bmatrix} \sigma_{11} \\ \sigma_{22} \\ \tau_{12} \end{Bmatrix}^{(k)} d\zeta \\
\{M\} &= \begin{Bmatrix} M_{11} \\ M_{22} \\ M_{12} \end{Bmatrix} = \sum_{k=1}^N \int_{\zeta_k}^{\zeta_{k+1}} \begin{Bmatrix} \sigma_{11} \\ \sigma_{22} \\ \tau_{12} \end{Bmatrix}^{(k)} \zeta d\zeta \\
\{Q\} &= \begin{Bmatrix} Q_2 \\ Q_1 \end{Bmatrix} = K_s \sum_{k=1}^N \int_{\zeta_k}^{\zeta_{k+1}} \begin{Bmatrix} \tau_{23} \\ \tau_{13} \end{Bmatrix}^{(k)} d\zeta
\end{aligned} \tag{7}$$

where the parameter  $K_s$  is the shear correction factor. Here,  $K_s$  is taken as 5/6.  $\zeta_k$  and  $\zeta_{k+1}$  are the coordinates of the upper and lower surfaces of the  $k$ th layer.

Substituting Eq. (4) into Eq. (7) and integrating through the thickness of the shell, the force and moment resultants are given in a compact form as

$$\begin{Bmatrix} \{N\} \\ \{M\} \end{Bmatrix} = \begin{bmatrix} [A] & [B] \\ [B] & [D] \end{bmatrix} \begin{Bmatrix} \{\varepsilon^0\} \\ \{\kappa\} \end{Bmatrix} \tag{8}$$

$$\{Q\} = K_s [A_s] \{\gamma\} \tag{9}$$

where  $[A]$ ,  $[B]$ ,  $[D]$  and  $[A_s]$  are defined by

$$\begin{aligned}
[A] &= \sum_{k=1}^N \int_{\zeta_k}^{\zeta_{k+1}} \overline{Q}_{ij}^{(k)} d\zeta & (i, j = 1, 2, 6) \\
[B] &= \sum_{k=1}^N \int_{\zeta_k}^{\zeta_{k+1}} \overline{Q}_{ij}^{(k)} \zeta d\zeta & (i, j = 1, 2, 6) \\
[D] &= \sum_{k=1}^N \int_{\zeta_k}^{\zeta_{k+1}} \overline{Q}_{ij}^{(k)} \zeta^2 d\zeta & (i, j = 1, 2, 6) \\
[A_s] &= \sum_{k=1}^N \int_{\zeta_k}^{\zeta_{k+1}} \overline{Q}_{ij}^{(k)} d\zeta & (i, j = 4, 5)
\end{aligned} \tag{10}$$

### 2.3 Equations of motions

The governing equations of motion of the first-order theory are derived using the dynamic version of the principle of virtual displacements (Reddy 2004)

$$\int_0^T (\delta U + \delta V - \delta K) dt = 0 \tag{11}$$

where  $T$  is the time limits,  $\delta K$  is the virtual kinetic energy of the system,  $\delta U$  is the virtual strain energy,  $\delta V$  is the virtual potential energy due to applied loads. The kinetic energy can be calculated by

$$\delta K = \int_V \rho [(\dot{u}_1)(\delta \dot{u}_1) + (\dot{u}_2)(\delta \dot{u}_2) + (\dot{u}_3)(\delta \dot{u}_3)] dV \quad (12)$$

where  $\rho$  is the mass density of the material.

The virtual strain energy of the shell can be written as

$$\delta U = \int_V \sigma_{ij} \delta \varepsilon_{ij} dV \quad (13)$$

Similarly, the virtual potential energy due to applied external loads is given by

$$\delta V = \int_A q \delta w_0 dA \quad (14)$$

where  $q$  is the load applied at the top surface of the shell.

Using Hamilton's principle, system of equations of motion of FSDT shell in the Cartesian coordinate system ( $x_1, x_2, x_3 = \zeta$ ) (note that  $N_{12} = N_{21} = N_6$  and  $M_{12} = M_{21} = M_6$ ) are obtained as (Reddy 2004)

$$\begin{aligned} \delta u_0 : \quad & \frac{\partial N_1}{\partial x_1} + \frac{\partial}{\partial x_2} (N_6 + C_0 M_6) + \frac{Q_1}{R_1} = I_0 \frac{\partial^2 u_0}{\partial t^2} + I_1 \frac{\partial^2 \Theta_1}{\partial t^2} \\ \delta v_0 : \quad & \frac{\partial}{\partial x_1} (N_6 - C_0 M_6) + \frac{\partial N_2}{\partial x_2} + \frac{Q_2}{R_2} = I_0 \frac{\partial^2 v_0}{\partial t^2} + I_1 \frac{\partial^2 \Theta_2}{\partial t^2} \\ \delta w_0 : \quad & \frac{\partial Q_1}{\partial x_1} + \frac{\partial Q_2}{\partial x_2} - \left( \frac{N_1}{R_1} - \frac{N_2}{R_2} \right) + q = I_0 \frac{\partial^2 w_0}{\partial t^2} \\ \delta \Theta_1 : \quad & \frac{\partial M_1}{\partial x_1} + \frac{\partial M_6}{\partial x_2} - Q_1 = I_1 \frac{\partial^2 u_0}{\partial t^2} + I_2 \frac{\partial^2 \Theta_1}{\partial t^2} \\ \delta \Theta_2 : \quad & \frac{\partial M_6}{\partial x_1} + \frac{\partial M_2}{\partial x_2} - Q_2 = I_1 \frac{\partial^2 v_0}{\partial t^2} + I_2 \frac{\partial^2 \Theta_2}{\partial t^2} \\ C_0 = & \frac{1}{2} \left( \frac{1}{R_1} - \frac{1}{R_2} \right) \end{aligned} \quad (15)$$

where  $I_0, I_1$  and  $I_2$  are mass moment inertia defined as

$$I_i = \sum_{k=1}^N \int_{\zeta_k}^{\zeta_{k+1}} \rho^{(k)}(\zeta)^i d\zeta \quad (i = 0, 1, 2) \quad (16)$$

### 2.4 Navier solution procedure

The simply supported boundary conditions (SS-1) for the first-order shear deformation shell theory are

$$\begin{aligned}
 u_1(x_1, 0, t) = 0, \quad u_1(x_1, b, t) = 0, \quad u_2(0, x_2, t) = 0, \quad u_2(a, x_2, t) = 0, \\
 N_1(0, x_2, t) = 0, \quad N_1(a, x_2, t) = 0, \quad N_2(x_1, 0, t) = 0, \quad N_2(x_1, b, t) = 0, \\
 \phi_1(x_1, 0, t) = 0, \quad \phi_1(x_1, b, t) = 0, \quad \phi_2(0, x_2, t) = 0, \quad \phi_2(a, x_2, t) = 0, \\
 u_3(x_1, 0, t) = 0, \quad u_3(x_1, b, t) = 0, \quad u_3(0, x_2, t) = 0, \quad u_3(a, x_2, t) = 0, \\
 M_1(x_1, 0, t) = 0, \quad M_1(x_1, b, t) = 0, \quad M_2(0, x_2, t) = 0, \quad M_2(a, x_2, t) = 0,
 \end{aligned} \tag{17}$$

The simply supported boundary conditions in Eq. (17) are satisfied by the following expansions of generalized displacement field

$$\begin{aligned}
 u_0(x_1, x_2, t) &= \sum_{n=1}^{\infty} \sum_{m=1}^{\infty} U_{mn}(t) \cos \alpha x_1 \sin \beta x_2 \\
 v_0(x_1, x_2, t) &= \sum_{n=1}^{\infty} \sum_{m=1}^{\infty} V_{mn}(t) \cos \alpha x_1 \sin \beta x_2 \\
 w_0(x_1, x_2, t) &= \sum_{n=1}^{\infty} \sum_{m=1}^{\infty} W_{mn}(t) \sin \alpha x_1 \sin \beta x_2 \\
 \varnothing_1(x_1, x_2, t) &= \sum_{n=1}^{\infty} \sum_{m=1}^{\infty} X_{mn}(t) \cos \alpha x_1 \sin \beta x_2 \\
 \varnothing_2(x_1, x_2, t) &= \sum_{n=1}^{\infty} \sum_{m=1}^{\infty} Y_{mn}(t) \sin \alpha x_1 \cos \beta x_2
 \end{aligned} \tag{18}$$

where  $\alpha = m\pi/a$ ,  $\beta = n\pi/b$ .

The mechanical loads are also expanded in double Fourier sine series

$$q(x_1, x_2, t) = \sum_{n=1}^{\infty} \sum_{m=1}^{\infty} Q_{mn}(t) \sin \alpha x_1 \sin \beta x_2 \tag{19}$$

where

$$Q_{mn}(t) = \frac{4}{ab} \int_0^a \int_0^b q(x_1, x_2, t) \sin \alpha x_1 \sin \beta x_2 dx_1 dx_2 \tag{20}$$

Analytical solution of the Eq. (15) can be obtained to simply supported cross-ply laminated shells (Reddy 1984). Towards using Navier type solution, first five partial differential equations are obtained in terms of mid-plane surface displacement ( $u_0$ ,  $v_0$ ,  $w_0$ ,  $\varnothing_1$ ,  $\varnothing_2$ ) by substituting the



force and moment resultants from Eqs. (8)-(9) into the system equations of motion (15). Substituting the expansions (18) and (19) into the five partially differential equations yields the equations

$$\begin{bmatrix} M_{11} & 0 & 0 & M_{14} & 0 \\ 0 & M_{22} & 0 & 0 & M_{25} \\ 0 & 0 & M_{33} & 0 & 0 \\ M_{41} & 0 & 0 & M_{44} & 0 \\ 0 & M_{52} & 0 & 0 & M_{55} \end{bmatrix} \begin{Bmatrix} U_{mn} \\ \dot{V}_{mn} \\ \ddot{W}_{mn} \\ \ddot{X}_{mn} \\ \dot{Y}_{mn} \end{Bmatrix} + \begin{bmatrix} K_{11} & K_{12} & K_{13} & K_{14} & K_{15} \\ K_{21} & K_{22} & K_{23} & K_{24} & K_{25} \\ K_{31} & K_{32} & K_{33} & K_{34} & K_{35} \\ K_{41} & K_{42} & K_{43} & K_{44} & K_{45} \\ K_{51} & K_{52} & K_{53} & K_{54} & K_{55} \end{bmatrix} \begin{Bmatrix} U_{mn} \\ V_{mn} \\ W_{mn} \\ X_{mn} \\ Y_{mn} \end{Bmatrix} = \begin{Bmatrix} 0 \\ 0 \\ Q_{mn} \\ 0 \\ 0 \end{Bmatrix} \quad (21)$$

where  $M_{ij}$  and  $K_{ij}$

$$M_{11} = M_{22} = M_{33} = I_0, \quad M_{14} = M_{25} = I_1, \quad M_{44} = M_{55} = I_2, \quad (22)$$

$$\begin{aligned} K_{11} &= A_{11}\alpha^2 + (A_{66} + 2C_0B_{66} + C_0^2D_{66})\beta^2 + \frac{K_s A_{SS}}{R_1^2} \\ K_{12} &= (A_{12} + A_{66} + C_0^2D_{66})\alpha\beta \\ K_{13} &= -\left[ \frac{1}{R_1}(A_{11} + K_s A_{SS}) + \frac{A_{12}}{R^2} \right] \alpha \\ K_{14} &= B_{11}\alpha^2 + (B_{66} + C_0D_{66})\beta_2 - \frac{K_s A_{SS}}{R_1} \\ K_{15} &= (B_{12} + B_{66} + C_0D_{66})\alpha\beta \\ K_{22} &= (A_{66} - 2C_0D_{66} + C_0^2D_{66})\alpha^2 + A_2\beta^2 + \frac{K_s A_{SS}}{R_2^2} \\ K_{23} &= -\left[ \frac{1}{R_1}A_{12} + \frac{1}{R_2}A_{22} + \frac{K_s A_{SS}}{R_2} \right] \beta \\ K_{24} &= (B_{12} + B_{66} - C_0D_{66})\alpha\beta \\ K_{25} &= (B_{66} - C_0D_{66})\alpha^2 + B_{22}\beta^2 - \frac{K_s A_{SS}}{R_1} \\ K_{33} &= K(A_{SS}\alpha^2 + A_{44}\beta^2) + \frac{A_{11}}{R_1^2} + \frac{2A_{12}}{R_1R_2} + \frac{A_2}{R_2^2} \\ K_{34} &= -\left( \frac{B_{11}}{R_1} + \frac{B_{12}}{R_2} \right) \alpha, \quad K_{35} = \left[ K_s A_{SS} - \left( \frac{B_{12}}{R_1} + \frac{B_{22}}{R_2} \right) \right] \beta \\ K_{44} &= (D_{11}\alpha^2 + D_{55}\beta^2 + K_s A_{SS}), \quad K_{45} = (D_{12} + D_{66})\alpha\beta \\ K_{55} &= (D_{66}\alpha^2 + D_{22}\beta^2 + K_s A_{44}) \end{aligned} \quad (23)$$

After simplification Eq. (21) can be written as follows

$$[M_{mn}]_{5 \times 5} \{\ddot{\Delta}_{mn}\}_{5 \times 1} + [K_{mn}]_{5 \times 5} \{\Delta_{mn}\}_{5 \times 1} = \{F_{mn}\}_{5 \times 1} \quad (24)$$

### 2.5 Laplace transforms of the governing equations

Application of Laplace transform with respect to time onto Eq. (24) yields

$$[\bar{D}_{mn}] \{\bar{\Delta}_{mn}\} = \{\bar{F}_{mn}\} + \{\bar{F}_0\} \quad (25)$$

where,  $\{\bar{\Delta}_{mn}\}$  and  $\{\bar{F}_{mn}\}$  are the transformed displacement vector and the transformed external force vector, respectively.  $[\bar{D}_{mn}]$  is the transformed dynamic stiffness matrix and  $\{\bar{F}_0\}$  is the initial condition force vector.  $[\bar{D}_{mn}]$  and  $\{\bar{F}_0\}$  are given as

$$[\bar{D}_{mn}] = [K_{mn}] + z^2 [M_{mn}] \quad (26)$$

$$\{\bar{F}_0\} = z [M_{mn}] \{\Delta(0)\} + [M_{mn}] \{\dot{\Delta}(0)\} \quad (27)$$

where  $z$  is the Laplace transform parameter.  $\{\Delta(0)\}$  is absolute initial displacement vector and  $\{\dot{\Delta}(0)\}$  is absolute initial velocity vector. Here, initial conditions are taken to be zero.

## 3. Numerical results and discussion

In this section, numerical analysis of simply supported (SS-1) cross-ply laminated composite shells based on FSDT subjected to suddenly-applied uniformly-distributed step load is presented. The numerical results are obtained with the suggested model and by using Navier approach combined with Newmark method. Verification of the presented procedure is performed by comparing with those obtained by finite element method (FEM) in conjunction with direct time integration technique. FEM in conjunction with direct time integration method results are calculated via ANSYS software. ANSYS software results of the laminated shells are obtained using  $(8 \times 8)$  mesh scheme. The mid-point deflection and the normal stress at the center of shell results are obtained and illustrated in figures. In all the examples, the deflection and normal stress ( $\zeta = -h/2$ ) at the mid-point of the laminated shell are showed in graphic forms. The normal stresses are calculated at the bottom surface ( $\zeta = -h/2$ ) of the shells.

In the example, the following layer properties are used.

Geometrical properties:  $a = b = 1$  m,  $h = 0.1$  m,  $R_1 = R_2 = R = 10$  m. ( $a/b = 1$ ,  $a/h = 10$ ).

Material properties:  $E_1 = 25 \times 10^9$  N/m<sup>2</sup>,  $E_2 = 1 \times 10^9$  N/m<sup>2</sup>,  $G_{12} = G_{13} = 0.5 \times 10^9$  N/m<sup>2</sup>,  $G_{23} = 0.2 \times 10^9$  N/m<sup>2</sup>,  $\nu = 0.25$  and  $\rho = 2,000$  kg/m<sup>3</sup>.

In the first case an anti-symmetric  $(0^\circ/90^\circ)$  laminated shell subjected to step load is considered. First a distributed load with the amplitude  $q_0 = 1000$  N/m<sup>2</sup> is applied suddenly on the laminated shell. Shell with  $(0^\circ/90^\circ)$  layers is first analyzed to confirm the present method. To achieve effect of the time increment, several Laplace transform parameters ( $N$ ) and time increment values ( $dt$ ) have been used. The mid-point deflection ( $w$ ) and the normal stress ( $\sigma_y$ ) for  $(0^\circ/90^\circ)$  laminates are presented in Fig. 2-3, respectively. Fig. 2 shows that the time-varying values of mid-point deflection achieved by the suggested method for different  $dt$  (0.00008, 0.00016, 0.00032, 0.00064)

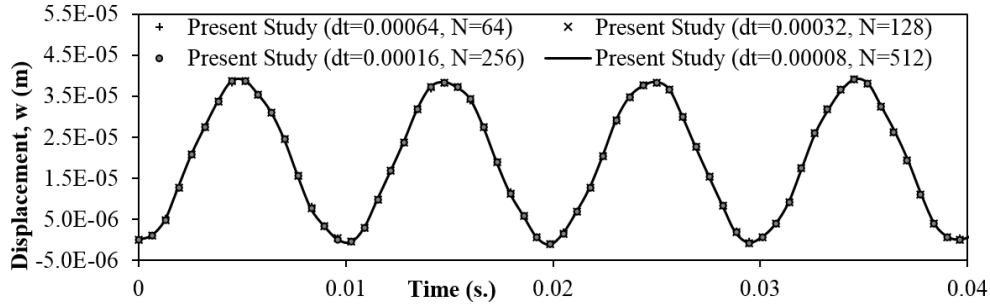


Fig. 2 Vertical displacement versus time for  $(0^\circ/90^\circ)$  laminates

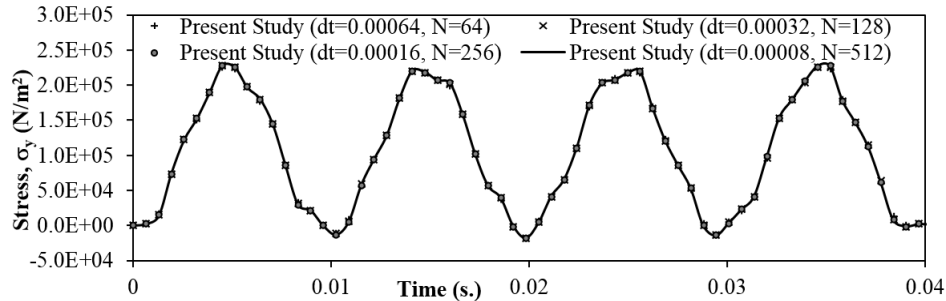


Fig. 3 Central stress versus time for  $(0^\circ/90^\circ)$  laminates

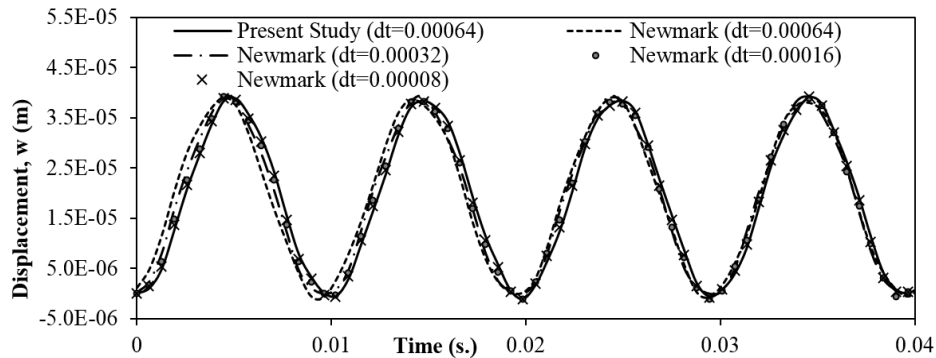


Fig. 4 Vertical displacement versus time for  $(0^\circ/90^\circ)$  laminates

and  $N$  (64, 128, 256, 512) are identical. Similarly, numerical results ( $\sigma_y$ ) at the bottom surface of the shell that are obtained with various time increments are identical (Fig. 3).

The mid-point deflection and the normal stress obtained with the aid of Navier solution combined with Newmark method are presented in Fig. 4-5, respectively. The vertical displacements and the normal stress obtained with the aid of finite element software ANSYS are presented in Fig. 6-7, respectively. Figs. 6 and 7 show that the time increments of 0.00008 and finer had to be considered for consistent results. An exact match is obtained by using a coarse time increment of 0.00064 in the present model as opposed to much finer increment of 0.00008 in the

Navier solution in conjunction with Newmark method and FEM in conjunction with the Newmark method (Fig. 4-7). Generally, the present method gives more accurate results when compared to other two methods aforementioned here.

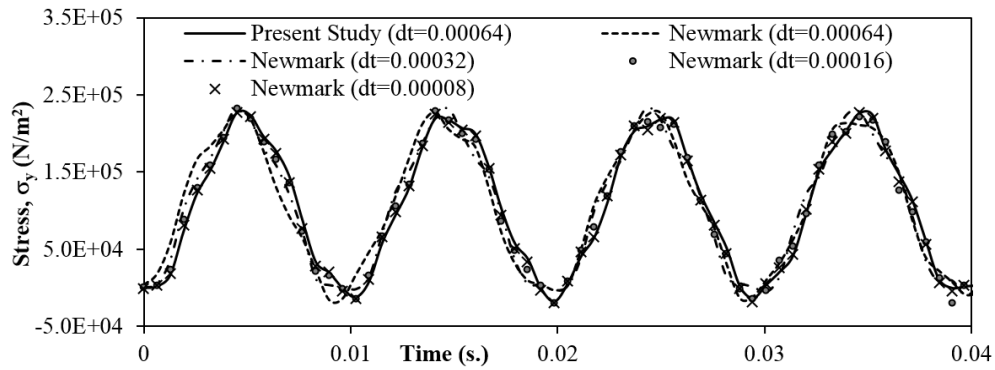


Fig. 5 Central stress versus time for (0°/90°) laminates

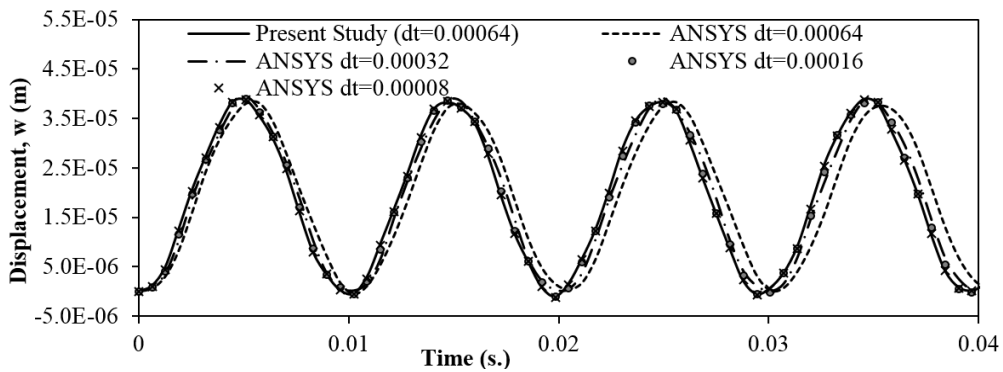


Fig. 6 Vertical displacement versus time for (0°/90°) laminates

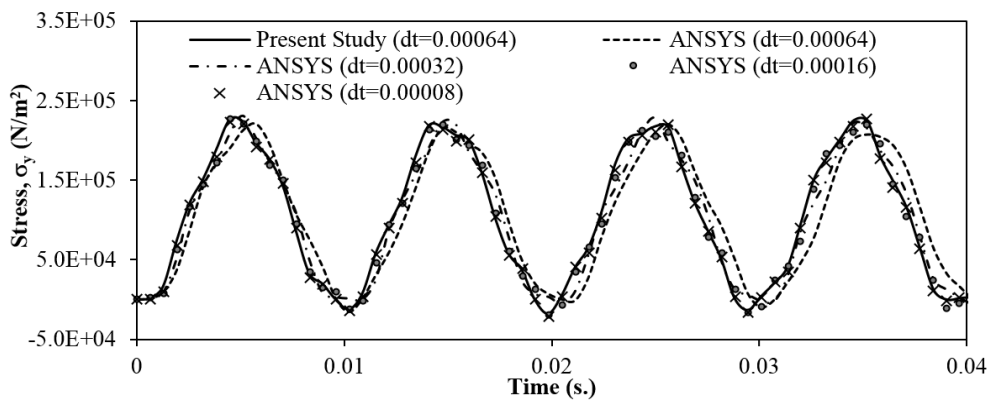


Fig. 7 Central stress versus time for (0°/90°) laminates

Second the triangular and rectangular impulsive loads are considered for  $(0^\circ/90^\circ)$  laminated shell. A distributed load with the amplitude  $q_0 = 1000 \text{ N/m}^2$  is applied on the laminated plate (See Fig. 8). In the impulsive load  $c$  is 0.02048 sec. The vertical displacement and central stress are shown in Figs. 9-10, respectively. It is seen that numerical results of vertical displacement and central stress obtained for various loads are convergent.

Having established reliabilities of the results obtained by the present method, numerical results of transient vibration analysis of orthotropic laminated shell are presented in the following figures.

The mid-point deflections obtained by various aspect ratios ( $a/h = 5, 10, 15, 20$ ) are presented

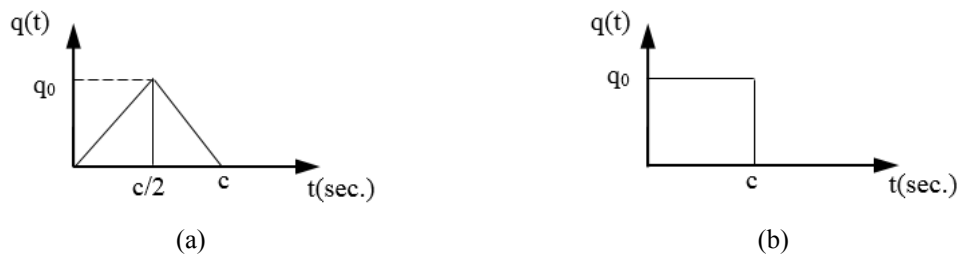


Fig. 8 Dynamic load: (a) rectangular impulse load (R); (b) triangular impulsive load (T)

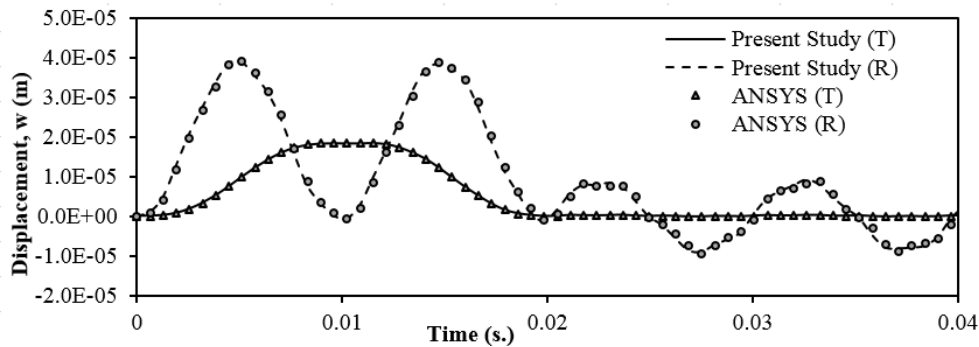


Fig. 9 Vertical displacement versus time for  $(0^\circ/90^\circ)$  laminates subjected rectangular impulse load (R), and triangular impulsive load (T)

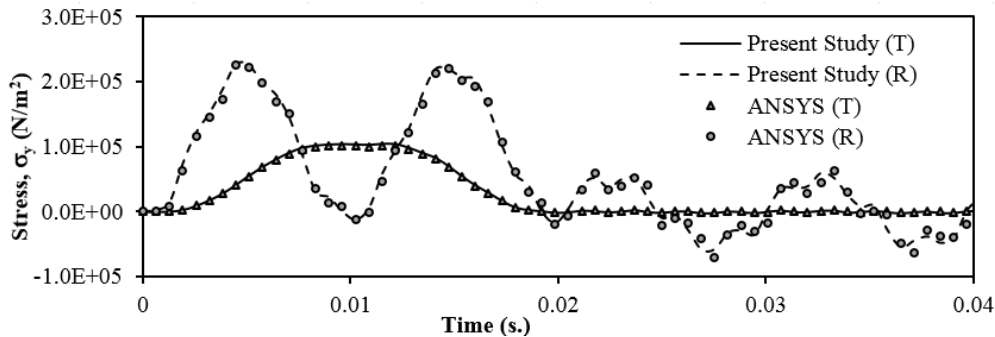


Fig. 10 Central stress versus time for  $(0^\circ/90^\circ)$  laminates subjected rectangular impulse load (R), and triangular impulsive load (T)

in Fig. 11. It shows that at a fixed value of curvature the change in the aspect ratio (with various  $h$ ) has a remarkable effect in the deflection for the thick cross-ply ( $0^\circ/90^\circ$ ) laminated shell. It can now be observed from Fig. 11 that by increasing the aspect ratio of cross-ply ( $0^\circ/90^\circ$ ) laminated shells, mid-point deflection amplitudes and periods are increased.

The mid-point virtual deflection for the various  $E_1/E_2$  ratio ( $E_1/E_2 = 1, 5, 10, 25, 50, 100$ ) are

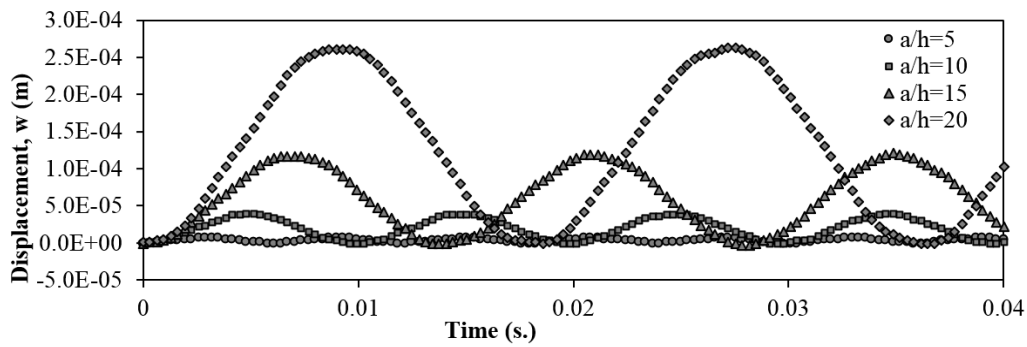


Fig. 11 Effect of aspect ratio for ( $0^\circ/90^\circ$ ) laminates

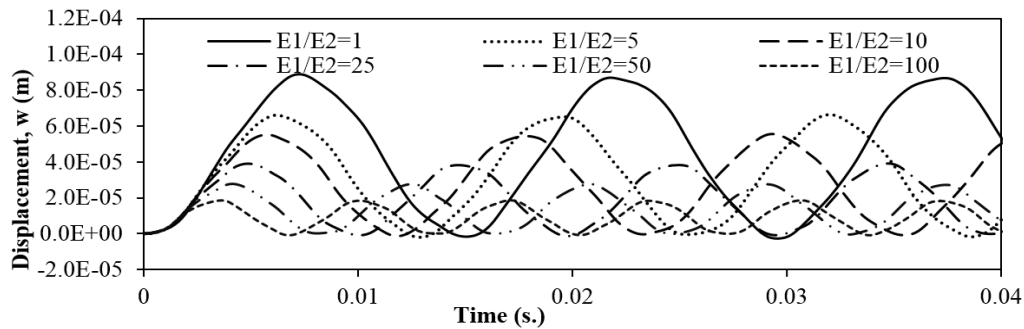


Fig. 12 Effect of  $E_1/E_2$  for ( $0^\circ/90^\circ$ ) laminates

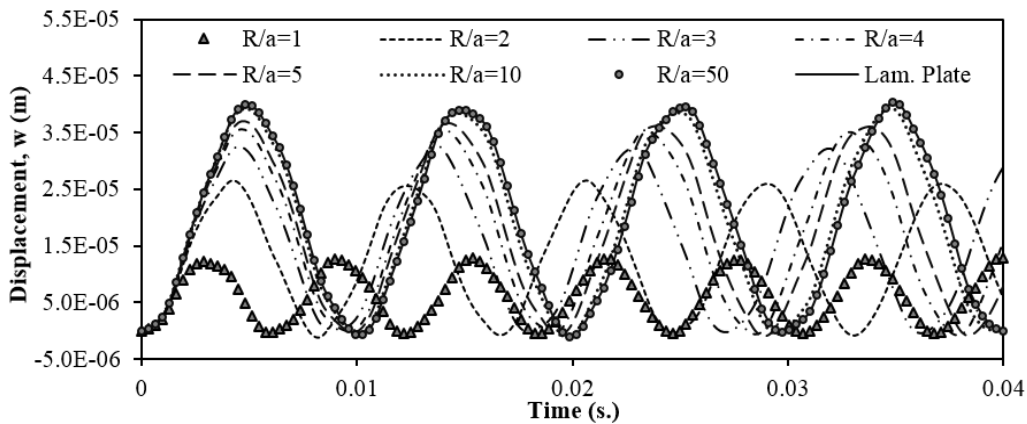


Fig. 13 Effect of geometric form for ( $0^\circ/90^\circ$ ) laminates

illustrated in Fig. 12. It is seen that at a fixed value of aspect ratio and curvature, the change in the  $E_1 / E_2$  ratio (with various  $E_2$ ) has a considerable effect on the deflection of the thick cross-ply ( $0^\circ/90^\circ$ ) laminated shell. It can be clearly seen that by increasing the  $E_1 / E_2$  ratio of laminated shells, mid-point deflection amplitudes and periods are decreased.

Fig. 13 presents the deflection according to geometric form which changes the curvature to length ( $R/a$ ) ratios. It shows that at a fixed value of thickness, the change in the curvature has a remarkable effect in the deflection for the thick cross-ply ( $0^\circ/90^\circ$ ) laminated shell when the curvature to length ratio has a small value. In other words, as the laminated shell becomes shallower the effect of changing  $R/a$  on changing the shell deflection becomes less important.

In Figs. 14-15, effect of number of layers on the transient vibration of laminated shell is investigated. Various shell structures are examined by choosing different number for  $(0^\circ/90^\circ)_k$  as  $k = 1, 2, 3, 4, 5$  and  $8$ . From Fig. 14 one can perceive that adding a layer and fixing shell thickness reduce the amplitudes and periods of deflection in cases with small number of layers. Also, figure clearly shows that adding a layer has not a considerable effect in the deflection for the thick anti-symmetric cross-ply  $(0^\circ/90^\circ)_k$  laminated shell when the number of layers is greater than 4 ( $k = 2$ ). As it can be seen increasing number of layers decreases amplitude and periods in a shell with

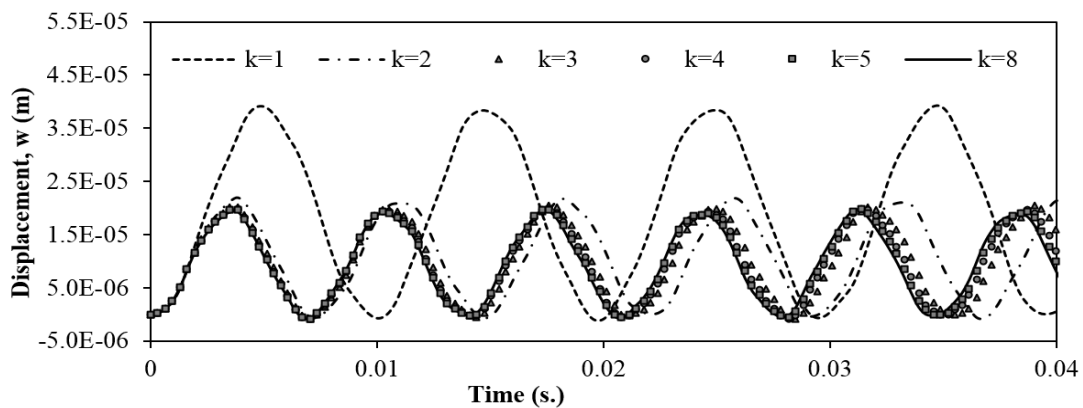


Fig. 14 Effect of ply-orientation for  $(0^\circ/90^\circ)_k$  laminates

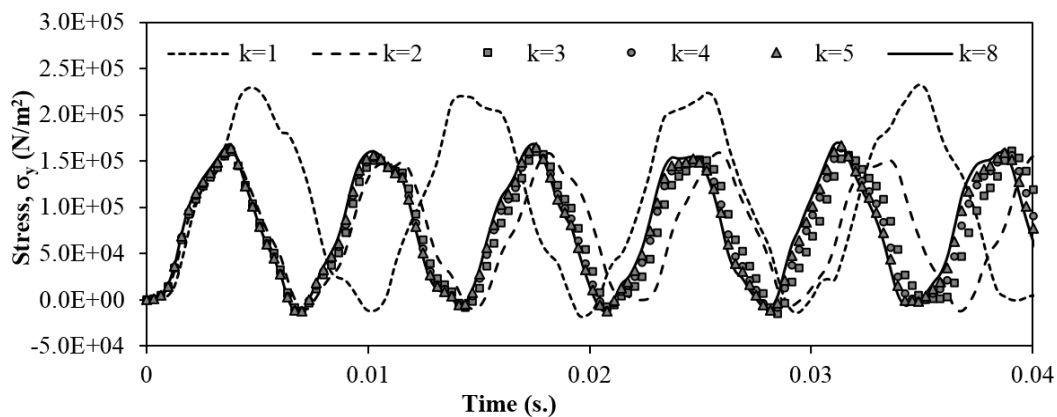
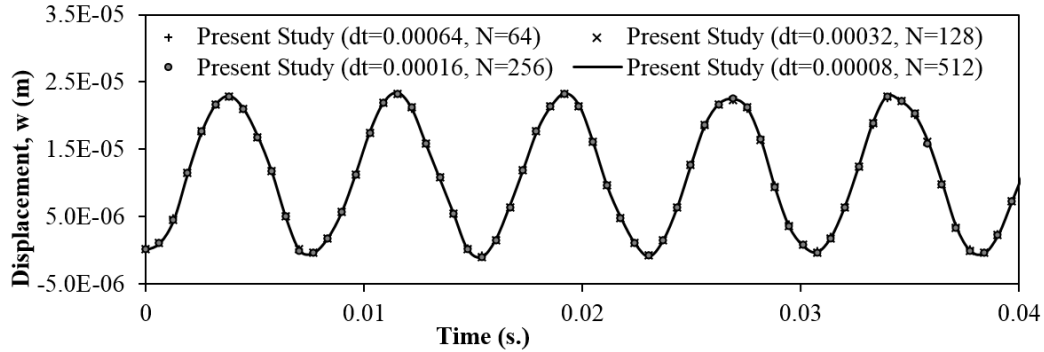
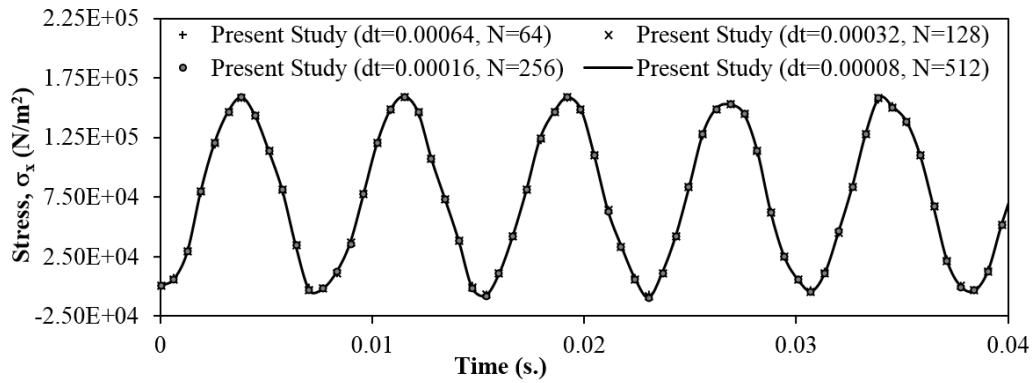


Fig. 15 Effect of ply-orientation for  $(0^\circ/90^\circ)_k$  laminates

Fig. 16 Vertical displacement versus time for  $(0^\circ/90^\circ/0^\circ)$  laminatesFig. 17 Central stress versus time for  $(0^\circ/90^\circ/0^\circ)$  laminates

$k = 1$  and 2; however, it has minimal effect in deflection with  $k = 3$  et seq.

Fig. 15 presents the normal stress with various number of layers. Similarly, the figure clearly shows that it has important effect with  $k = 1$  and 2, but not so with  $k = 3$  et seq.

In the second case  $(0^\circ/90^\circ/0^\circ)$  laminated shell subjected to a step load is considered. The mid-point deflection ( $w$ ) and the central normal stresses ( $\sigma_x$ ) of the shell obtained with presented method are shown in Fig. 16-17, respectively. Similarly, numerical results of  $(0^\circ/90^\circ/0^\circ)$  laminated shell for various time increments are identical.

#### 4. Conclusions

By increasing the aspect ratio of cross-ply laminated shells, mid-point deflection amplitudes and periods are increase. By increasing the  $E_1//E_2$  ratio of laminated shells, mid-point deflection amplitudes and periods are decrease. As the  $E_2$  ratio of laminated shells, mid-point deflection amplitudes and periods are decrease. As the laminated shell becomes shallower the effect of changing  $R/a$  on changing the shell deflection becomes less important. Adding layers does not have a considerable effect on the deflection for the thick anti-symmetric cross-ply  $(0^\circ/90^\circ)_k$  laminated shell when the number of layers is greater than 4 ( $k = 2$ ). Application of Laplace



transform reduces dynamic problem to a static one, which is solved numerically in the Laplace domain. In addition, it should be noted that natural frequencies and mode shapes are not needed in the solutions. The accuracy of the results of Newmark method depends on the time increment selection. Thus, the choice of the optimum time increment cannot be left to chance. In the method examined here, however, even a coarse time increment gives highly accurate results. It is clear that the suggested procedure is much more efficient than the conventional step-by-step integration methods. The numerical results have proved that the present approach is a highly accurate and effective solution method when compared to other direct integration methods.

## Acknowledgments

The authors thank Adiyaman University Scientific Research Projects Directorate that supported the present work (MUFBAP/2014-0002).

## References

- Brigham, E.O. (1974), *The Fast Fourier Transform*, Prentice-Hall, Inc., Englewood Cliffs, NJ, USA.
- Chun, L. and Lam, K.Y. (1995), "Dynamic analysis of clamped laminated curved panels", *Compos. Struct.*, **30**(4), 389-398.
- Civalek, O. (2006), "Free vibration analysis of composite conical shells using the discrete singular convolution algorithm", *Steel Compos. Struct., Int. J.*, **6**(4), 353-366.
- Correia, I.F.P., Barbosa, J.I. and Mota, C.A. (2000), "A finite element semi-analytical model for laminated axisymmetric shells: statics, dynamics and buckling", *Comput. Struct.*, **76**(1-3), 299-317.
- Dogan, A. and Arslan, H.M. (2012), "Investigation of the effect of shell plan-form dimensions on mode-shapes of the laminated composite cylindrical shallow shells using SDSST and FEM", *Steel Compos. Struct., Int. J.*, **12**(4), 303-324.
- Durbin, F. (1974), "Numerical inversion of Laplace transforms: An efficient improvement to Dubner and Abate's method", *Comput. J.*, **17**(4), 371-376.
- Fares, M.E., Youssif, Y.G. and Alamir, A.E. (2003), "Minimization of the dynamic response of composite laminated doubly curved shells using design and control optimization", *Compos. Struct.*, **59**(3), 369-383.
- Ganapathi, M., Patel, B.P. and Pawargi, D.S. (2002), "Dynamic analysis of laminated cross-ply composite non-circular thick cylindrical shells using higher-order theory", *Int. J. Solids Struct.*, **39**(24), 5945-5962.
- Gong, S.W., Shim, V.P.W. and Toh, S.L. (1995), "Impact response of laminated shells with orthogonal curvatures", *Compos. Eng.*, **5**(3), 257-275.
- Her, S.-C. and Liang, Y.-C. (2004), "The finite element analysis of composite laminates and shell structures subjected to low velocity impact", *Compos. Struct.*, **66**(1-4), 277-285.
- Jung, W.-Y. and Han, S.-C. (2014), "Transient analysis of FGM and laminated composite structures using a refined 8-node ANS shell element", *Compos. Part B Eng.*, **56**, 372-383.
- Krishnamurthy, K.S., Mahajan, P. and Mittal, R.K. (2001), "A parametric study of the impact response and damage of laminated cylindrical composite shells", *Compos. Sci. Technol.*, **61**(12), 1655-1669.
- Krishnamurthy, K.S., Mahajan, P. and Mittal, R.K. (2003), "Impact response and damage in laminated composite cylindrical shells", *Compos. Struct.*, **59**(1), 15-36.
- Lee, Y.S., Choi, M.H. and Kim, J.H. (2003), "Free vibrations of laminated composite cylindrical shells with an interior rectangular plate", *J. Sound. Vib.*, **265**(4), 795-817.
- Li, J. and Hua, H. (2009), "Transient vibrations of laminated composite cylindrical shells exposed to underwater shock waves", *Eng. Struct.*, **31**(3), 738-748.
- Narayanan, G.V. (1979), "Numerical operational methods in structural dynamics", Ph.D. Thesis, University

- of Minnesota, Minneapolis, MN, USA.
- Park, T., Kim, K. and Han, S. (2005), "Linear static and dynamic analysis of laminated composite plates and shells using a 4-node quasi-conforming shell element", *Compos. Part B. Eng.*, **37**(2-3), 237-248.
- Prusty, B.G. and Satsangi, S.K. (2001), "Finite element transient dynamic analysis of laminated stiffened shells", *J. Sound Vib.*, **248**(2), 215-233.
- Reddy, J.N. (1984), "Exact solutions of moderately thick laminated shells", *J. Eng. Mech.*, **110**(5), 794-809.
- Reddy, J.N. (2004), *Mechanics of laminated composite plate and shells: theory and analysis*, (Second Ed.), CRC Press, Boca Raton, FL, USA.
- Sahan, M.F. (2012), "Dynamic analysis of viscoelastic composite plates in the Laplace domain", Ph.D. Thesis, University of Cukurova, Adana, Turkey.
- Saviz, M.R. and Mohammadpourfard, M. (2010), "Dynamic analysis of a laminated cylindrical shell with piezoelectric layers under dynamic loads", *Finite Elem. Anal. Des.*, **46**(9), 770-781.
- Shim, V.P.W., Toh, S.L. and Gong, S.W. (1996), "The elastic impact response of glass/epoxy laminated ogival shells", *Int. J. Impact Engng.*, **18**(6), 633-655.
- Sofiyev, A.H. (2003), "Torsional buckling of cross-ply laminated orthotropic composite cylindrical shells subject to dynamic loading", *Eur. J. Mech. - A/Solids*, **22**(6), 943-951.
- Swaddiwudhipong, S. and Liu, Z.S. (1997), "Response of laminated composite plates and shells", *Compos. Struct.*, **37**(1), 21-32.
- Temel, B. (2003), "Transient analysis of viscoelastic helical rods subject to time-dependent loads", *Int. J. Solids Struct.*, **41**(5-6), 1605-1624.
- Temel, B. and Şahan, M.F. (2013), "An alternative solution method for the damped response of laminated Mindlin plates", *Compos. Part B. Eng.*, **47**, 107-117.
- Temel, B. and Şahan, M.F. (2013), "Transient analysis of orthotropic viscoelastic thick plates in the Laplace domain", *Eur. J. Mech. - A/Solid*, **37**, 96-105.
- Timarci, T. and Soldatos, K.P. (2000), "Vibrations of angle-ply laminated circular cylindrical shells subjected to different sets of edge boundary conditions", *J. Eng. Math.*, **37**(1-3), 211-230.
- Toh, S.L., Gong, S.W. and Shim, V.P.W. (1995), "Transient stresses generated by low velocity impact on orthotropic laminated cylindrical shells", *Compos. Struct.*, **31**(3), 213-228.
- Topal, U. (2013), "Pareto optimum design of laminated composite truncated circular conical shells", *Steel Compos. Struct., Int. J.*, **14**(4), 397-408.
- Vaziri, R., Quan, X. and Olson, M.D. (1996), "Impact analysis of laminated composite plates and shells by super finite elements", *Int. J. Impact Eng.*, **18**(7-8), 765-782.
- Wu, C.-P., Tarn, J.-Q. and Chi, S.-M. (1996), "An asymptotic theory for dynamic response of doubly curved laminated shells", *Int. J. Solids Struct.*, **33**(26), 3813-3841.

## Appendix

The analysis of the differential equations governing the behavior of the system are carried out in the Laplace domain and the Modified Durbin's algorithm based on the Fast Fourier Transform (FFT) sub-program (Brigham 1974), is used for the inversion of the results back to time domain. This algorithm is developed from Durbin's numerical inverse Laplace transform method (Durbin 1974). Durbin's algorithm formula are given by

$$f(t_j) \cong \frac{2e^{aj\Delta t}}{T} \left[ -\frac{1}{2} \operatorname{Re}\{\bar{F}(a)\} + \operatorname{Re}\left\{ \sum_{k=0}^{N-1} (A(k) + iB(k)) e^{\left(i\frac{2\pi}{N}\right)jk} \right\} \right] \quad (\text{A1})$$

$$A(k) = \sum_{l=0}^L \operatorname{Re}\left\{ \bar{F}\left(a + i(k + lN)\frac{2\pi}{T}\right) \right\} \quad (\text{A2})$$

$$B(k) = \sum_{l=0}^L \operatorname{Im}\left\{ \bar{F}\left(a + i(k + lN)\frac{2\pi}{T}\right) \right\} \quad (\text{A3})$$

where,  $i$  is the complex number,  $T$  is sampling time interval,  $N$  is the total number of equidistant sampling points ( $N = 2^m$ ;  $m$  being integer),  $z_k = a + ik2\pi/T$  is  $k$ th Laplace transform parameter,  $t_j = j\Delta t = jT/N$ , ( $j = 0, 1, 2, \dots, N-1$ ). In Eq. (1), the second part of the equality between the brackets is

$$\left\{ \sum_{k=0}^{N-1} (A(k) + iB(k)) e^{\left(i\frac{2\pi}{N}\right)jk} \right\} \quad (\text{A4})$$

calculated by using a Fast Fourier Transform sub-program Eq. (A1) can also be modified according to the Narayanan's suggestion (Narayanan 1979).

$$f(t_j) \cong \frac{2e^{aj\Delta t}}{T} \left[ -\frac{1}{2} \operatorname{Re}\{\bar{F}(a)\} + \operatorname{Re}\left\{ \sum_{k=0}^{N-1} (\bar{F}(z_k) L_k) e^{\left(i\frac{2\pi}{N}\right)jk} \right\} \right] \quad (\text{A5})$$

where, each term of discrete values that is calculated in the Laplace domain is modified by multiplying them with Lanczos ( $L_k$ ) factor. These factors are given by

$$L_k : \begin{cases} = 1, & k = 0 \\ = \sin\left(\frac{k\pi}{N}\right) / \left(\frac{k\pi}{N}\right), & k > 0 \end{cases} \quad (\text{A6})$$

It should be noted that, the selection of the appropriate values of parameters  $N$ ,  $a$  and  $T$  are critical in order to achieve the desired accuracy in the inverse transform. In the literature it is indicated that setting the value of  $T$  and choosing the value of  $a$  multiplied by  $T$  ( $aT$ ) in between  $5 \leq aT \leq 10$  yields the value of  $a$  necessary for the required precision (Durbin 1974). For the numerical examples showed in this study the value of ' $aT$ ' is taken as '6'.